Microphase Separation and Wetting Properties of Palmitate-*graft*-poly(vinyl alcohol) Films

C. Biver,* G. de Crevoisier,† S. Girault, A. Mourran,‡ R. Pirri,§ J. C. Razet, and L. Leibler

UMR 167, ESPCI-CNRS-ATOFINA, 10 rue Vauquelin, 75231 Paris Cedex 05, France

Received March 27, 2001; Revised Manuscript Received September 27, 2001

ABSTRACT: Bulk and surface organization properties of grafted copolymers having an hydrophilic poly(vinyl alcohol) backbone and hydrophobic palmitic side chains were investigated. A structural study shows the existence of a microphase separation into lamellar structures for grafting ratios of only 0.09. Water wettability of films obtained by solvent casting from these grafted copolymers indicates a good segregation and organization of the alkyl chains at the surface of the films even at grafting ratio as low as 0.04. The quality of the solvent used during the copolymer film formation is shown to have a strong influence on organization and wetting properties of these materials. The existence of specific interactions of H-bond type in the PVA phase seems to be responsible for a strong incompatibility between the hydrophilic backbone and the hydrophobic side chains leading to such surprisingly good bulk and surface organizations.

Introduction

A large number of technologically important applications of polymeric materials require to control the level of surface hydrophilicity or hydrophobicity. Depending on the application, one may require that a given liquid wets the polymer surface (adhesion, printing, etc.) or, at the opposite, beads up on a repellent polymer surface (waterproofing, oil or soil repellency, etc.).

Various methods have been developed to control the wetting behavior of polymer surfaces. That goal may be achieved by external surface treatments and/or by surface modifications induced by a bulk restructuration of multicomponent polymeric systems.[1] External surface treatments include chemical and physical methods such as acid etching, flame treatment, plasma treatment, UV irradiation, etc., and may be combined with the surface grafting of new molecules or macromolecules onto the top of the initial polymer surface. Multicomponent polymeric materials are particularly interesting since surface modifications can be induced by a reorganization of the surface, in particular due to a change in its environment. For example, low molecular weight additives are often used since they are able to diffuse from the bulk toward the surface of the polymer material. Similar effects can be observed in films made of block copolymers or grafted chains where blocks or pendant groups can reorientate on the surface exposing hydrophilic or hydrophobic moieties. Chemical compatibility, molecular mobility of components, and molecular architecture are among the main parameters that control surface wettability of such materials.

A considerable theoretical and experimental effort has been devoted to understand the structuring and surface properties of polymer blends[2] and block copolymers.[3−6] Much less is known about grafted copolymers[7,8] and even less about copolymers able to crystallize. Yet, such systems could exhibit unique features since they can organize both on a very local scale (crystallization) and on a mesoscopic scale (microphase separation).[9,10] One can ask the question how such a system could organize in a bulk phase. For low incompatibility between the grafts and the backbone, a homogeneous phase can be a priori expected (Figure 1a). In the completely opposite limit of very incompatible grafts regularly spaced along the backbone, a very regular mesophase with both the backbone and the side chains crystallized could occur (Figure 1b). In intermediate situations and polydispersed systems in which grafts are not regularly spaced, less organized structures could exist.

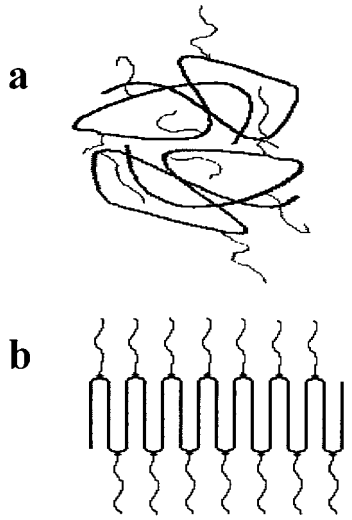

Figure 1. Two possible organizations of grafted copolymers where both the backbone and the side chains are able to crystallize. (a) Coil conformation in the homogeneous phase. (b) Crystallization of the backbone and of the side chains in separated domains. In practice, intermediate cases where either the backbone or the side chains crystallize could also be expected.

The aim of this paper is to study an example of such a system, namely an amphiphilic grafted copolymer consisting of a hydrophilic poly(vinyl alcohol) backbone

† Present address: ATOFINA Japan, Kyoto Technical Center SCB#3, Kyoto Research Park, 1 Awatacho, Chudoji, Shimigyo-ku Kyoto 600-8815 Japan.

‡ Present address: Makromolecular Chemie, Universitat Ulm, 89069 Ulm, Germany.

§ ATOFINA, Groupement de recherches de Lacq, BP 34, 64170 Lacq, France.

* To whom correspondence should be addressed.

10.1021/ma010526j CCC: $22.00
Published on Web 02/23/2002

onto which hydrophobic palmitic side chains are randomly attached. The general formula of the synthesized grafted copolymers may be written as $[CH_2-CH(OH)]_{1-X}$-$[CH_2-CH(OCO(CH_2)_{14}CH_3)]_X$ with X, the grafting ratio, ranging from 0.015 to 0.17.

We discuss both bulk organization and surface properties of these materials and show that by varying the number of side chains per chain we are able to control both the bulk structure and the wettability of the surface. A spectacular result is that depending on the conditions of surface film formation and on the environment we can get either hydrophilic or hydrophobic materials. The paper is organized as follows:

In section II we describe the materials and experimental methods used in this study. Next, we discuss the observed structures and demonstrate the existence of a microphase separation between alkyl chains domains and PVA domains. The important result here is that a crystallization of either the side chains or the backbone can occur depending on the grafting ratio. From classical theories of microphase separation in amorphous grafted copolymers,[11] one would expect no microphase separation for molecular architecture studied here. Our observations thus tend to show that specific interactions along the polymer backbone and crystallization of both segments could lead to microphase separation. In section IV, we show that the surface wetting properties of these materials, particularly their water sensitivity, are very dependent on their bulk organization. A crystallization of hydrophobic side chains appears necessary to get the more hydrophobic material with the lowest water sensitivity. Finally, in section V, we demonstrate that depending on the conditions of surface film formation and on the environment, we can get either hydrophilic or hydrophobic materials.

Experimental Section

Materials. Palmitic chains were grafted on poly(vinyl alcohol) (PVA) by partial esterification of PVA with acid chloride in homogeneous phase as described by Arranz et al.[12] The used PVA is a commercial product, Rhodoviol 4.20 from Rhone Poulenc. Its number-average molecular weight is 27 000 with a polydispersity index of 1.2 and an hydrolysis degree of 98% as given by the supplier. Palmitoyl chloride (Aldrich) is used as received. PVA is dissolved in *N*-methyl-2-pyrrolidone (NMP) (Fluka) at 80−90 °C in a reactor equipped with a dry N_2 flow to prevent any contact with water vapor. Then the solution is cooled to room temperature, and pyridine is added as a catalyst. Palmitoyl chloride is added dropwise under vigorous agitation. After 16 h reaction at room temperature the polymer is precipitated in diethyl ether and then thoroughly washed with diethyl ether and water until all residual NMP, pyridine, and palmitoyl chloride or acid are removed. Then all the copolymer samples are dried at 50 °C under vacuum and characterized by NMR spectroscopy. The grafting ratio X ranges from 1.5 to 17 mol % with respect to the total number of hydroxyl and ester groups as determined from ^{1}H NMR in d_6-DMSO. A statistical distribution of the palmitic side chains is obtained for $X = 0.17$ as seen by ^{13}C NMR in a d_6-DMF/DMF mixture.

Film Preparation. Copolymers were dissolved at a concentration of 10 wt % in DMSO which is a good solvent for the PVA and the alkyl chains.

Thick films (∼100 μm) were prepared for structural studies by casting the copolymer solutions at room temperature with a very low evaporation rate under dry nitrogen for several days. Films are finally dried at 50 °C under vacuum to remove the solvent completely.

Thinner films (∼5 μm) for wetting studies were obtained by coating glass microscope coverslides (24 × 30 mm^2) as follows: Glass coverslides are cleaned by soaking in sulfochromic acid for 1 h, thoroughly rinsed with ultrapure water (Milli Q-185 Plus), and finally dried in an oven for 6 h. Films are formed by dipping these coverslides for 1 h into the copolymer solutions. The coverslides are then slowly removed at a constant velocity of 0.4 mm/min and dried directly at 50 °C under vacuum in a vertical position to remove slowly and completely the DMSO.

Indeed, DMSO is well-known for its water affinity and can absorb water from the atmosphere, thus reducing solvent quality for the alkyl chains and affecting film formation. The influence of solvent quality was checked by letting the coated coverslides for 24 h at room temperature under ambient relative humidity before the final drying at 50 °C under vacuum.

Film Characterization. *Bulk Structure.* X-ray diffraction and small-angle X-ray scattering were used to study structure variations in thicker films at size scale ranging from about 1 to 300 Å. Observations were performed in transmission mode by using a Cu Kα radiation (1.54 Å) from an X-ray rotating anode generator (RU-200, Rigaku Ltd.) operated at 40 kV and 30 mA. Wide-angle diffracted intensity was collected between 3° and 120° using a curved position-sensitive detector (CPS 120, Inel). Small-angle scattered intensity was measured with a linear detector (LPS 50, Inel) and film-to-detector distance of 315 mm.

Surface Tension. The Wilhelmy plate method was used to measure advancing and receding contact angles of water on the copolymer-coated coverslides.[13] Measurements were performed at 25 °C by moving the plate up and down in the water at 0.4 mm/min using a Lauda tensiometer. Surface tension of water was measured before and after contact with the copolymer coatings to check whether no copolymer was dissolved during the measurements.

Surface Topography. The surface roughness and coating thickness were measured by atomic force microscopy (AFM) using a Dimension 3000 (Digital Instruments, Inc., Santa Barbara, CA) operated in contact or in tapping mode with a G-type scan head (maximum scan range 90 × 90 μm^2). The measurements were carried out in air under normal conditions.

Images obtained with the height mode and a 512 × 512 dots resolution in the XY horizontal plane are presented. The mean surface roughness, R_a, was calculated on these images according to the following formula. R_a is defined as the mean value of the surface height relative to a center plane calculated so that the above and below delimited volumes are equal.

$$R_a = \frac{1}{L_x L_y}\int_0^{L_y}\int_0^{L_x} |f(x,y)|\, dx\, dy$$

where $f(x,y)$ is the surface relative to the center plane and L_x and L_y are the dimensions of the scanned area.

All measurements were performed at ambient temperature, pressure, and relative humidity unless specified.

Results and Discussion

Structural Organization in Copolymer Films. This section deals with the characterization of the bulk structural organization of the grafted PVA's as a function of the grafting ratio X of hydrophobic palmitic chains on the hydrophilic poly(vinyl alcohol) backbone. We first describe the structure deduced at very small length scales (∼1−25 Å) from wide-angle X-ray diffraction (WAXD) experiments; then we discuss results concerning the existence of a microphase separation, as observed from small-angle X-ray scattering (SAXS) experiments. WAXD and SAXS curves for grafted PVA with $X = 0.015$ are not presented in the following; they appear to be similar to the ones of raw PVA, indicating no major change of the small and long-range organiza-

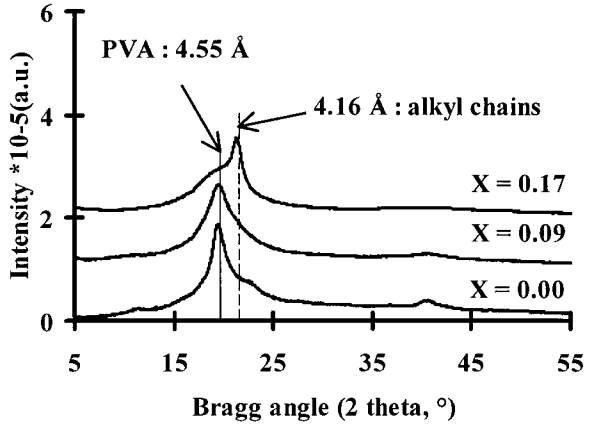

Figure 2. Wide-angle X-ray scattered intensity vs Bragg angle (2θ, deg) curves as a function of the grafting ratio X. Note that the intensity scale is correct for $X = 0$. Baselines have been shifted upward for $X = 0.09$ and 0.17 for curves differentiation.

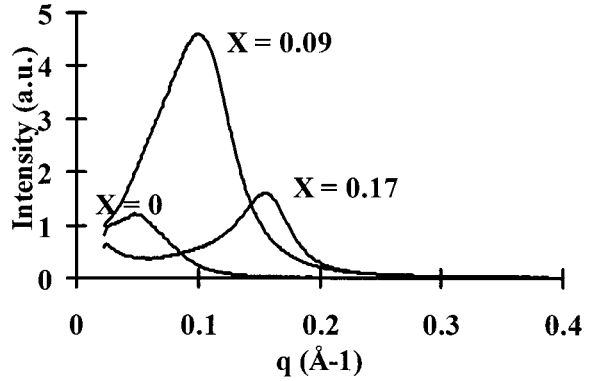

Figure 3. Small-angle X-ray scattered intensity vs wave vector (q, Å^{-1}) curves for nonmodified PVA and for grafted PVA with $X = 0.09$ and $X = 0.17$.

Table 1. Characteristic Spacings for PVA and Grafted PVA

grafting ratio X	vol fraction of alkyl chains[a]	Bragg spacing (Å)	L (Å) from q_{max}	L (Å) from Porod law	$l_b + l_{sc}$ (Å)
0	0	4.55	137		
0.015	0.11	4.55	137		
0.09	0.43	4.55	63	56	59
0.17	0.59	4.16	41	41	48

[a] Volume fractions have been calculated for the different grafting ratios assuming mean densities of alkyl chains and poly(vinyl alcohol) of 0.83 and 1.20 g cm^{-3}, respectively.

tion for this very low grafting ratio. More interesting results are observed for $X = 0.09$ and 0.17. In these samples the volume fraction occupied by the alkyl chains is 0.43 and 0.59, respectively. The corresponding WAXD and SAXS curves are shown in Figures 2 and 3, along with those for PVA.

WAXD. The Bragg spacings associated with the main diffraction peak are listed in Table 1. For $X = 0$, 0.015, and 0.09 this peak is located at 4.55 Å and can be attributed to the distance between lattice plane $(10\bar{1})$ of crystalline PVA domains[14] in monoclinic structure. When X increases from 0 to 0.09, the domain size of these PVA domains, estimated from the broadness of the peak according to the Scherrer formula,[15] decreases from about 300 to 200 Å. At the same time, the organization of the alkyl chains increases. Indeed, for $X = 0.17$ the main diffraction peak at 4.16 Å is found very close to the one obtained for palmitic acid (strongest line d_{hkl} at 4.10 Å in a monoclinic structure[16]) and for hexadecylpolyacrylate (strongest line d_{110} at 4.19 Å with an hexagonal structure[17]) and is associated with the characteristic spacing between planes of alkyl chains in quite well-ordered domains.

SAXS. A typical SAXS curve of a semicrystalline polymer is observed for the raw PVA ($X = 0$). The q-position of the intensity maximum may be related to a long period of about 140 Å as indicated in Table 1 and the scattered intensity to the difference in electronic density between amorphous and crystalline phase in PVA domains (~0.05 electron mol cm^{-3}). For $X = 0.09$ and 0.17, the scattered intensity I is much higher. Its variation vs q is faster than the q^2 prediction of Benoit and Hadziioannou[11] for homogeneous grafted copolymers, suggesting a microphase separation. Figure 4 shows the existence of a plateau in the q^4I vs q representation after the background correction suggested by Koberstein.[18] This q^4 dependence as well as the Ruland representation[18] (Figure 4 inset) clearly indicates the existence of a sharp interface (thickness ~ 10 Å) between domains of different electronic density inside the films and hence probes the microphase separation. Indeed, this interface thickness appears smaller than the one found by Mao et al.[19] for liquid crystal−coil diblock copolymers having a polystyrene block and azobenzene side groups. In addition, the increase in scattered intensity from raw PVA to grafted PVA certainly reflects the increase in electronic density contrast when passing from raw PVA to grafted PVA where the contrast is due to the difference between PVA and alkyl chains (~0.15 to 0.33 electron mol cm^{-3}). Since the volume fractions of PVA and alkyl chains are about equal, we expect these systems to be organized in lamellar phase. To confirm this hypothesis, we determine the mean period L of this lamellar structure by two independent methods, either from the maximum of the SAXS peak or from the Porod plateau. The two values presented in Table 1 are in good agreement and appear compatible with a lamellar structure. The period L equals the sum of the mean distance between grafting points along PVA backbone (l_b) and twice the length of the alkyl side chains ($l_{sc} \cong 16.4$ Å) (cf. Table 1). Therefore, SAXS and WAXS results suggest an organization in the phase separated domains as illustrated in Figure 5 for $X = 0.09$ and $X = 0.17$. At low volume fraction in alkyl chains, PVA crystallization dominates the process of phase separation, while at volume fraction higher than 0.5, the alkyl chains crystallize, preventing PVA crystallization. In addition, almost no intensity is scattered near zero angle, suggesting rather wide organized domains.

Actually, according to existing theories[11] for amorphous grafted copolymers A-*g*-B and reasonable χ_{AB} parameters, our grafted copolymers should exhibit only homogeneous phases. Wang et al.[20] observed phase separation and lamellar organization with fluorinated side chains ionenes having a greater χ_{AB}. In our case, the ability of either the backbone or the side chains to crystallize, together with the existence of specific interactions of H-bond type along the backbone, seems to be at the origin of the observed phase separation. It would be interesting to perform complementary studies on PVA grafted with lower alkyl chains or on grafted poly(vinyl acetate) to precise this point.

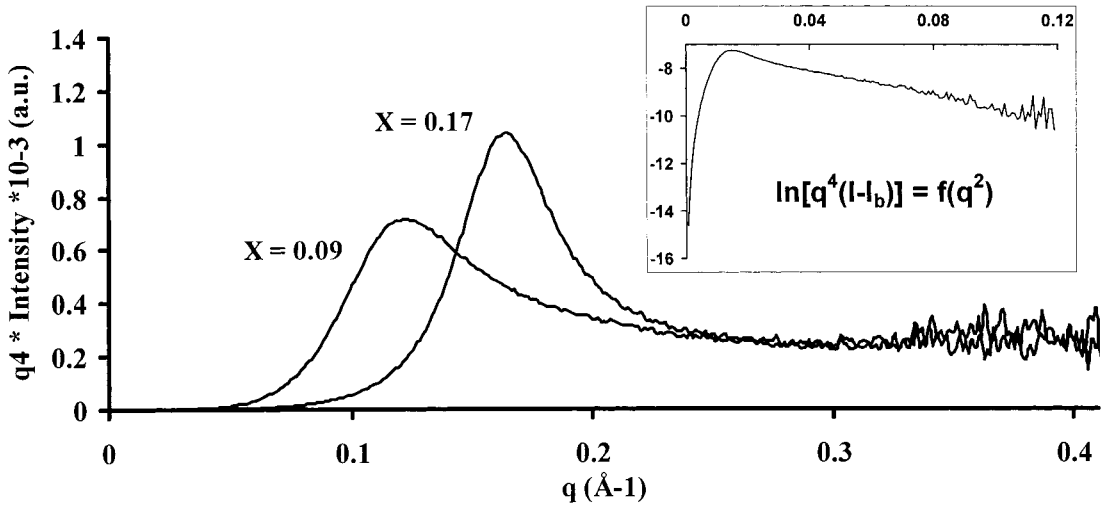

Figure 4. Porod representation ($q^4I = f(q)$) for the grafted PVA samples with $X = 0.09$ and 0.17. Inset: Ruland representation[18] $\ln(q^4(I - I_b) = f(q^2)$ for $X = 0.09$. The background intensity, I_b, has been approximated to an exponential at wide q according to $I_b = F_1 \exp(bq^2)$. The slope of the curve for $0.04 < q^2 < 0.12$ yields a thickness of the interface of the order of 10 Å.

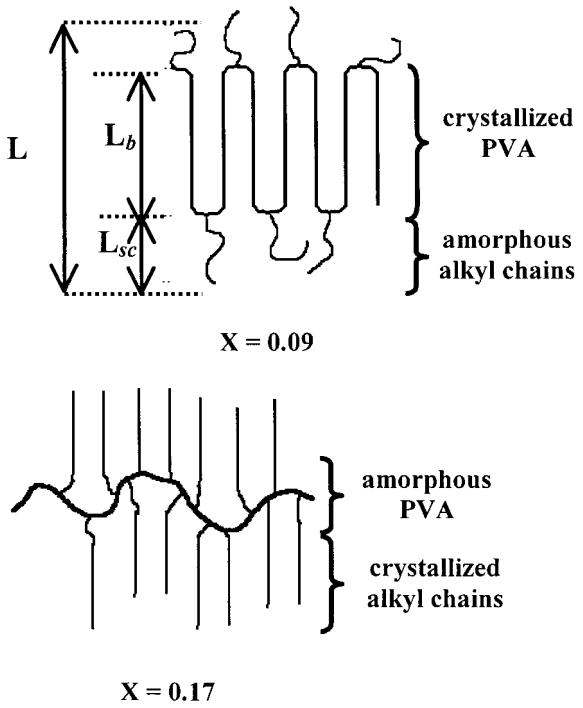

Figure 5. Model representation of the organized domains in grafted PVA films for $X = 0.09$ and $X = 0.17$.

In the next section we examine how this bulk organization influences the surface properties by investigating wetting properties on thin films dried directly under vacuum.

Wetting Properties. Figure 6 shows the variations of the advancing (θ_a) and receding (θ_r) contact angles of water on grafted-PVA coatings as a function of X. The surface tension of the water used for these measurements has been checked before the experiments (γ_l = 72 mN/m) and was found to decrease from 72 to 65 mN/m for the nonmodified PVA and for the grafted PVA with $X = 0.015$ after three dipping cycles of the coating in water, indicating a partial solubility of these two polymers in water at room temperature during the duration of the experiment (about 2 h). Surprisingly, even for this small grafting ratio the advancing contact angle ($\theta_a \sim 114°$) is much higher than with pure PVA ($\theta_a \sim 55°$).

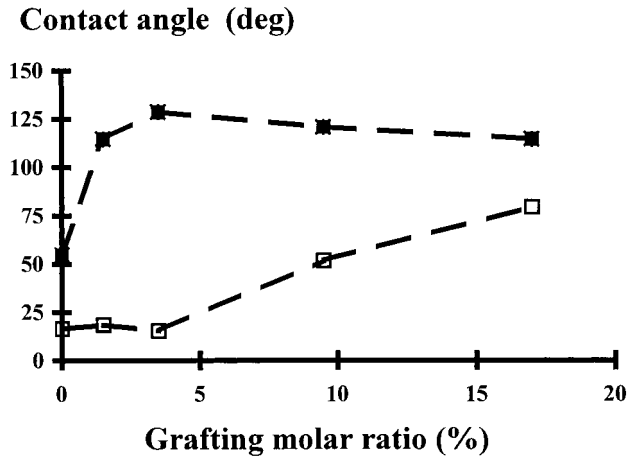

Figure 6. Advancing and receding contact angles of water on grafted poly(vinyl alcohol) coatings dried under vacuum as a function of the grafting ratio X (full square, θ_a; open square, θ_r).

For X higher than 0.02, the surface tension of water, γ_l, remains constant, indicating that no copolymer was released from the coating during the measurements. As the grafting ratio increases, the advancing contact angle, θ_a, seems to pass through a maximum around $X = 0.04$ and then decreases slowly. On the contrary, the receding contact angle, θ_r, remains very low and almost constant (about 16°) at a value corresponding to pure PVA as long as $X < 0.04$. Then θ_r increases up to 80° for $X = 0.17$, showing the hydrophobic character of the copolymer film surface.

A comparison with homopolymers confirms the good organization of the grafts at the surface. Indeed, Kasemura et al.[21] have reported θ_a and θ_r values of the same order of magnitude for poly(vinyl palmitate) homopolymer, i.e., $X = 1$ at the same dipping velocity.

The high θ_a value, we observed for a very low grafting ratio, is in favor of a strong segregation and organization of the alkyl chains at the surface and may be related to the bulk phase separation observed in the previous section.

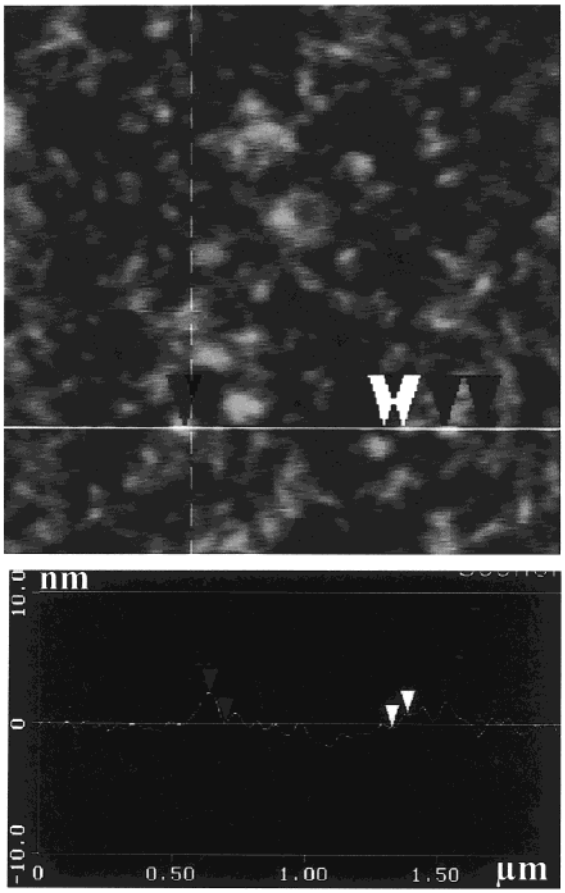

Figure 7. (a) 2 × 2 μm^2 AFM micrograph of the coating surface topology for grafted poly(vinyl alcohol) with $X = 0.09$, directly dried under vacuum. (b) Cross-sectional profile along the line drawn in the topography image.

The contact angle hysteresis $\Delta\theta$, defined as the difference between the advancing and receding angles, is rather high ($\Delta\theta \sim 110°$) near $X = 0.04$ but decreases slowly down to around 34° at $X = 0.17$. Many effects could in principle be at the origin of the observed contact angle hysteresis.[22,23] A very common source of hysteresis is a presence of impurities (dust) at the film surface. To eliminate it, we have taken special care during preparing, drying, and studying the coatings. The surface roughness and/or chemical heterogeneities at the surface of the film can also lead to the contact angle hysteresis.[24,25] Indeed, as the coating advances in water (or water spreads on the coating), the triple contact line tends to be stopped ("anchored") by either the asperities or the low-wetting hydrophobic patches on the surface, leading to a higher apparent advancing contact angle. Similarly, once the entire surface has been covered by water during the advancing step, the valleys or the high-energy hydrophilic zones will prevent water from receding.

To determine an eventual role of the surface roughness, we have examined the surface by atomic force microscopy (AFM). Figure 7 shows a 2 × 2 μm^2 AFM image of the surface topography of a coating prepared from grafted PVA with $X = 0.09$. The surface presents some steps whose higher depth is lower than 3 nm. The mean surface roughness is very small, only 0.6 nm. This value is negligible compared to that usually considered as having an effect on hysteresis ($R_a > 100$ nm).[22]

In our experiments, the hysteresis appears to be time dependent, suggesting that dipping in water is responsible for surface modification. We observe a decrease in the advancing and receding contact angles as the number of cycles in water increases. At the same time the hysteresis increases (Table 2). Clearly, the surface becomes more hydrophilic. Actually, in the presence of water, polar groups of the copolymer can orientate toward the water/polymer interface and thus decrease the interfacial tension.[20,26−28] For instance, Takara et al.[29] observed surface reorganization for segmented poly(ether−urethane−ureas) in contact with water with poly(ethylene glycol) as the polyether component. For more hydrophilic polymers an appreciable swelling of the film surface layer is even possible.[30] As a result, the film surface after having been in contact with water becomes more hydrophilic, and so the receding contact angle decreases. For even more hydrophilic copolymers, the polymer may be partially soluble in water, leading to a decrease of the surface tension of water as observed above for $X = 0$ and $X = 0.015$. As a consequence, the apparent receding angle also decreases.

Table 2. Contact Angles of Water on a Coating of a Grafted PVA[a] with $X = 0.09$, Directly Dried under Vacuum; 1, 2, and 3 Refer to the Number of Dipping Cycles in to and out of Water at a Velocity of 0.4 mm/min

wetting cycles in water	θ_{adv} (deg)	θ_{rec} (deg)	$\Delta\theta$ (deg)
1	121	52	69
2	122	32	91
3	118	23	95

[a] The AFM topography images 7 and 8 were obtained on this coating on areas which has not been into water (Figure 7) and which has been three times into water (Figure 8).

We have investigated the effect of successive dipping cycles in to and out of water on the topography of the copolymer film surface for $X = 0.09$. After the third cycle, the film has been dried at room temperature in the presence of air and its surface examined by AFM. The comparison of Figure 8 with Figure 7 clearly shows that dipping the film into water affects the topography of the film surface. The number and depth of asperities have increased appreciably after the film has been dipped into water. Their presence suggests a partial swelling of the film surface in water. Still the surface roughness remains very small (0.9 nm), too small to induce such a strong hysteresis. Hence, we are tempted to conclude that the observed hysteresis is mainly due to the restructuration of the water/polymer interface both by a reorientation of polar hydroxyl group and by water penetration. Such a surface reconstruction may also increase the "chemical" heterogeneity of the surface and thus increase the hysteresis. It is important to stress that hysteresis effects are strongly reduced for the most hydrophobic copolymer with $X = 0.17$ (cf. Table 3). The good ordering of the alkyl side chains, demonstrated by the bulk structural study presented in section III, prevents easy surface reconstruction, and the overall hydrophobicity of copolymers reduces the film swelling.

Macrophase Separation at Copolymer Film Surfaces. In contrast with the above studies where the films have been dried under vacuum, the grafted PVA coatings examined here have been let evaporate slowly, the coverslides in a vertical position, for 24 h at room temperature in the presence of air and at ambient relative humidity, before being dried under vacuum to remove completely the DMSO.

During the drying in air, a whitening of the coatings is observed. Topography images realized at different heights on the coverslide coated with the grafted PVA

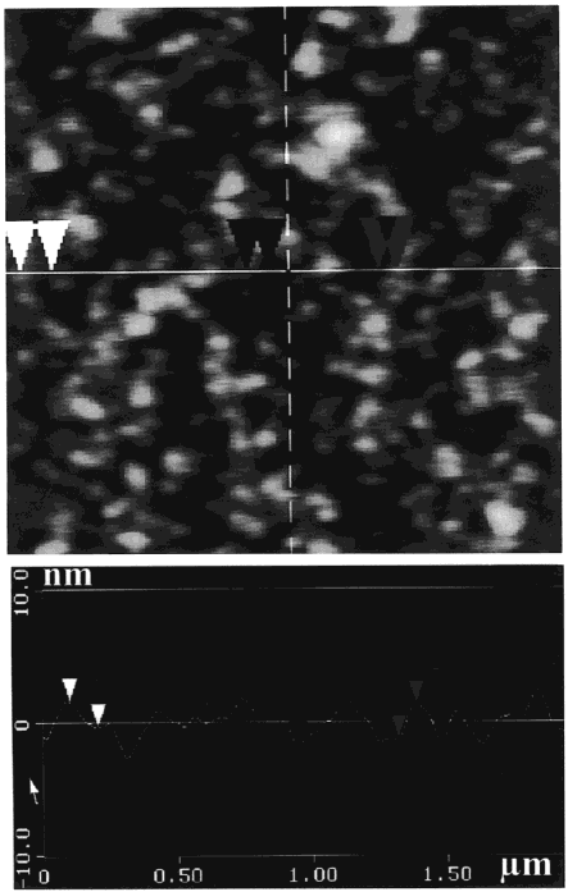

Figure 8. (a) 2 × 2 μm^2 AFM micrograph of the coating surface of Figure 7 after three successive dippings in water. (b) Cross-sectional profile along the line drawn in the topography image.

Table 3. Contact Angles of Water on a Coating of the Grafted PVA with $X = 0.17$, Directly Dried under Vacuum, as a Function of the Number of Dipping in to and out of Water (Dipping Velocity 0.4 mm/min)

wetting cycles in water	θ_{adv} (deg)	θ_{rec} (deg)	$\Delta\theta$ (deg)
1	114	79	35
2	111	78	33

having $X = 0.09$ are shown in Figure 9a−c from the top to the bottom. Figure 9a shows the existence of big holes with a radial symmetry at the film surface after complete solvent evaporation. This surface topography is clearly different from the one obtained by drying the coating directly under vacuum, i.e., in absence of humidity (see Figure 7). The hole size is large, typically of the order of 2 μm in diameter and 200 nm in depth, and explains the whitening of the films.

This phenomenon is observed on thicker films (∼200 μm) prepared by casting a solution of copolymer in DMSO in the presence of air under relative humidity and is attributed to a macrophase separation. This macrophase separation certainly originates from a change in solvent quality at the surface due to water absorption by DMSO during its slow evaporation. Indeed, as mentioned in the Experimental Section, DMSO, which is a quite good solvent for poly(vinyl alcohol) and alkyl chains, is well-known for its water affinity. As soon as water is absorbed, solvent quality is reduced for alkyl chains, and macrophase separation occurs, leading to the formation of high- and low-viscosity macroscopic domains with radial symmetry at

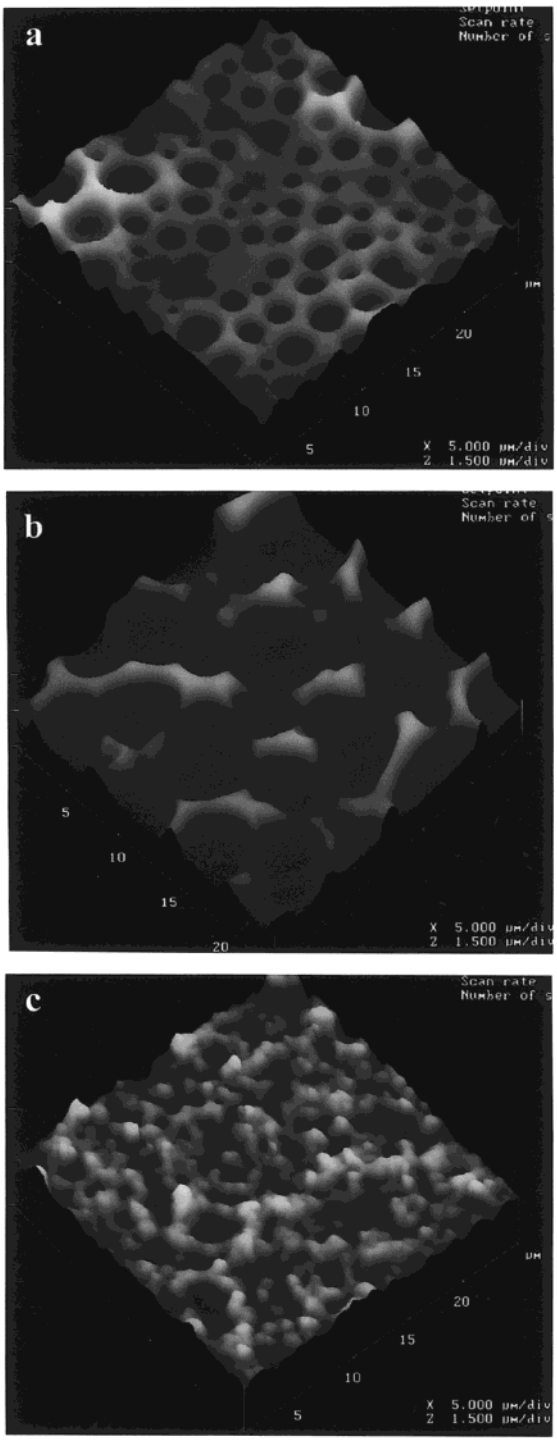

Figure 9. 25 × 25 μm^2 AFM micrographs showing the dewetting of a film of poly(vinyl alcohol) grafted with 9 mol % of palmitic chains coated on glass and dried in the presence of humidity in a vertical position: (a) Top of the coating. (b) Middle of the coating. (c) Bottom of the coating. The depth and diameter of the holes in (a) are of about 200 and 2000 nm, respectively.

the film surface, attributed to "copolymer in DMSO" rich zones and "DMSO plus water" zones, respectively. After complete solvent evaporation, the "DMSO plus water" zones are replaced by the holes observed on Figure 9a−c. Such macrophase separation can be completely avoided by drying the film directly under vacuum or nitrogen to avoid contact with water vapor.

This macrophase separation appeared to be time and film thickness dependent. The variation in hole dimen-

sions from the top to the bottom of the coating illustrates the combined effect of time and thickness. Because of drainage, the thickness of the film decreases from the top to the bottom. As a consequence, the drying of the film, associated with solvent evaporation, is faster at the top and phase separation is quenched in an earlier stage when the phase separated domains are still relatively small. In the middle of the coating, the phase separation can proceed further. The increase in hole size between (a) and (b) results from a coarsening of the domains under line tension effect which tends to reduce interfaces in order to minimize surface free energy. The bottom of the holes in Figure 9b is formed by a flat copolymer film. The mean roughness at the bottom of the coating is of the order of 80 nm on a surface of $25 \times 25\ \mu m^2$ (Figure 9c) that is much higher than the 0.6 nm measured on films directly dried under vacuum. This phenomenon of holes formation has been used recently to prepare controlled patterned polymer surfaces.[31]

Macrophase Separation and Wetting Properties. When contact angles against water are measured on a surface such as the one shown in Figure 9c, the advancing value is comparable and sometimes slightly higher than the one on film dried directly under vacuum; on the contrary the receding angle is always smaller. For instance, in the case of $X = 0.09$, θ_a and θ_r values of 128° and 0°, respectively, are obtained. The small increase in roughness can explain the slight increase in θ_a. After dipping into water, water may be retained by capillary forces by this rougher surface, thus explaining that θ_r is zero. After being in contact with water and dried at air, surface roughness still increases slightly up to 140 nm. Surface chemical composition may also be different as observed by Yuan[32] with poly(trifluorovinyl ether)/polystyrene blends films depending on the casting solvent. AFM observation of the film surface under water would be informative of the real surface topography and rugosity during contact angle measurements.

Indeed, the topography of the surfaces shown in Figure 9 is analogous to the one obtained during the phenomena of phase separation and dewetting of polymer surfaces. Most of the polymer phase separation and dewetting studies reported in the literature concern polymer blends,[33,34] grafted polymer brushes, microphase-separated block copolymers,[35−37] or grafted copolymers bearing mesogenic side groups.[38] In this last case, dewetting is activated by a change in temperature. At low temperature the organization of the mesogenic groups tends to microphase separate the copolymer, hence balancing the coiling tendency of the backbone. Dewetting is shown to occur above the isotropisation temperature of the mesogenic groups.

In our case, dewetting at the copolymer surface can be induced by the phase separation process associated with the change in solvent quality. When films as in Figure 9c are dipped into water, penetration of water in the PVA domains at the outermost surface can start such a dewetting process and/or a partial swelling of the film, leading to the surface roughness increase.

In conclusion, it seems that solvent quality and drying conditions used to make a coating strongly influence the topography of the films and its wetting properties.

Conclusion

A bulk microphase separation between PVA and alkyl chains domains and a good organization of the alkyl chains at the polymer film surfaces is found from X-ray scattering and wetting studies on films made of palmitic chain-*graft*-poly(vinyl alcohol) with grafting ratio lower than 17 mol %. This behavior, unusual for copolymers grafted with short side chains and at low grafting ratios, is attributed to a strong incompatibility between the hydrophilic and hydrophobic segments reinforced by specific attractive interactions (H bonds) in the PVA phase. Because of the polar nature of the backbone, below 10 mol % grafting ratio, polymer film surfaces still have significant water sensitivity which lead to water contact-time-dependent contact angles, the main causes for this being surface swelling and group reorientation. At 17 mol % of palmitic chains, water sensitivity is greatly reduced, and wetting properties become similar to those of poly(vinyl palmitate) homopolymer. In addition, it has been shown that the quality of the solvent used during the copolymer film formation has a strong influence on its organization and wetting properties. A good solvent for both the backbone and the side chains leads to the best wetting properties, while a bad solvent for the side chains can induced macrophase separation and surface roughness.

Acknowledgment. The authors thank J. P. Lallier for insightful discussions on DMSO properties and all their colleagues who contributed to the copolymer characterization.

References and Notes

(1) Garbassi, F.; Morra, M.; Ochiello, E. *Polymer Surfaces, From Physics to Technology*; J. Wiley & Sons: New York, 1998.
(2) Kumacheva, E.; Li, L.; Winnik, M. A.; Shinozaki, D. M.; Cheng, P. C. *Langmuir* **1997**, *13*, 2483.
(3) Bates, F. S.; Fredrickson, G. H. *Annu. Rev. Phys. Chem.* **1990**, *41*, 525.
(4) Nakahama, S.; Hirao, A.; Mori, H.; Senshu, K. *Polym. Prepr.* **1995**, *36*, 57.
(5) Hamley, I. W.; Fairclough, J. P. A.; Terrill, N. J.; Ryan, A. J.; Lipic, P. M.; Bates, F. S.; Towns-Andrews, E. *Macromolecules* **1996**, *29*, 8835.
(6) Wang, J.; Mao, G.; Ober, C. K.; Kramer, E. J. *Macromolecules* **1997**, *30*, 1906.
(7) Qiu, Y.; Yu, X.; Feng, L.; Yang, S. *Chin. J. Polym. Sci.* **1995**, *13*, 112.
(8) Dozier, W. D.; Peiffer, D. G.; Lin, M. Y.; Rabeony, M.; Thiyagarajan, P.; Behal, S. K.; Disko, M. M. *Int. J. Polym. Anal. Charact.* **1995**, *1*, 259.
(9) Yao, Y.; Liu, L.; Li, H.; Fang, T.; Zhou, E. *Polymer* **1994**, *35*, 14.
(10) Mathis, A.; Le Moigne, J.; Gramain, P. *Eur. Polym. J.* **1973**, *9*, 283.
(11) Benoit, H.; Hadzioannou, G. *Macromolecules* **1988**, *21*, 1449.
(12) Arranz, F.; Sanchez Chaves, M.; Gil, F. *Angew. Makrom. Chem.* **1980**, *92*, 121.
(13) Adamson, A. W. *Physical Chemistry of Surface*; Wiley-Interscience: New York, 1990.
(14) Matsumoto, T.; et al. *Kobunshi Kagaku (Chemistry of High Polymers)* **1971**, *28*, 315, 610.
(15) Guinier, A. Théorie et Technique de la Radiocristallographie, Dunod, 1956.
(16) JCPDS-ICDD database, 1995, 24-1853.
(17) Platé, N. A.; Sibaev, V. P.; Petrukhin, B. S.; Zubov, Yu. A.; Kargin, V. A. *J. Polym. Sci.* **1971**, *9*, 2291.
(18) Koberstein, J. T.; Morra, B.; Stein, R. S. *J. Appl. Crystallogr.* **1980**, *13*, 34. Ruland, W. *J. Appl. Crystallogr.* **1971**, *4*, 70.
(19) Mao, G.; Wang, J.; Clingman, S. R.; Ober, C. K.; Chen, J. T.; Thomas, E. L. *Macromolecules* **1997**, *30*, 2556.
(20) Wang, J.; Ober, C. K. *Macromolecules* **1997**, *30*, 7560.
(21) Kasemura, T.; Takahashi, S.; Nakane, N.; Maegawa, T. *Polymer* **1996**, *37*, 3659.
(22) Johnson, R. E.; Dettre, R. *Surface Colloid Sci.* **1969**, *2*, 85.
(23) de Gennes, P. G. *Rev. Mod. Phys.* **1985**, *57*, 3, 827.
(24) Johnson, R. E.; Dettre, R. *Adv. Chem.* **1964**, *43*, 112.
(25) Drelich, J.; Wilbur, J. L.; Miller, J. D.; Whitesides, G. M. *Langmuir* **1996**, *12*, 1913.

(26) Shanahan, M. E. R.; Carre, A.; Moll, S.; Schultz, J. *J. Chim. Phys.* **1986**, *83*, 35.
(27) Ruckenstein, E.; Gourisankar, S. V. *J. Colloid Interface Sci.* **1985**, *107*, 488.
(28) Yasuda, H.; Sharma, A. K. *J. Polym. Sci.* **1981**, *19*, 1285.
(29) Takahara, A.; Jo, N. J.; Kajiyma, T. *J. Biomater. Sci., Polym. Ed.* **1989**, *1*, 17.
(30) Sedev, R. V.; Petrov, J. G.; Neumann, A. W. *J. Colloid Interface Sci.* **1996**, *180*, 36.
(31) Mourran, A.; Sheiko, S. S.; Krupers, M.; Möller, M. *Polym. Mater. Sci. Eng.* **1999**, *80*, 175.
(32) Yuan, Y.; Shoichet, M. S. *Macromolecules* **2000**, *33*, 4926.
(33) Ermi, B. D.; Nisato, G.; Douglas, J. F.; Rogers, J. A.; Karim, A. *Phys. Rev. Lett.* **1998**, *81*, 3900. Nisato, G.; Ermi, B. D.; Douglas, J. F.; Karim, A. *Macromolecules* **1999**, *32*, 2356.
(34) Müller-Buschbaum, P.; Gutmann, J. S.; Stamm, M. *Macromolecules* **2000**, *33*, 4886.
(35) Leibler, L.; Mourran, A. *MRS Bull.* **1997**, Jan, 33.
(36) Yerushalmi-Rozen, R.; Klein, J. *Langmuir* **1995**, *11*, 2806.
(37) Heier, J.; Sivaniah, E.; Kramer, E. J. *Macromolecules* **1999**, *32*, 9007.
(38) Sheiko, S.; Lermann, E.; Möller, M. *Langmuir* **1996**, *12*, 4015.

MA010526J